



Contents lists available at ScienceDirect

# Remote Sensing Applications: Society and Environment



journal homepage: [www.elsevier.com/locate/rsase](http://www.elsevier.com/locate/rsase)



## Multispectral UAV data for detection of weeds in a citrus farm using machine learning and Google Earth Engine: Case study of Morocco

Hajar Saad El Imanni <sup>a,\*</sup>, Abderrazak El Harti <sup>a</sup>, El Mostafa Bachaoui <sup>a</sup>, Hicham Mouncif <sup>a</sup>, Fatine Eddassouqui <sup>a</sup>, Mohamed Achraf Hasnai <sup>b</sup>, Moulay Ismail Zinelabidine <sup>c</sup>

<sup>a</sup> Geomatics, Georesources and Environment Laboratory, Faculty of Sciences and Techniques, Sultan Moulay Slimane University, Beni Mellal, Morocco

<sup>b</sup> FarmAssist 360, Beni Mellal, Morocco

<sup>c</sup> Exploitation Manager, Beni Mellal, Morocco

### ARTICLE INFO

#### Keywords:

Weed mapping  
Multispectral UAV imagery  
Google earth engine (GEE)  
Machine learning  
Canopy height model (CHM)

### ABSTRACT

Accurate and timely weed mapping between and within trees is considered one of the major challenges in the site-specific weed management systems. This research presents the first cloud computing approach based on the incorporation of multispectral Unmanned Aerial Vehicle (UAV) imagery in the Google Earth Engine (GEE) programming environment with the aim of improving the mapping of weed patches between and within trees in a citrus farm. For this purpose, the UAV multispectral bands (red, green, blue, near infrared, and red edge), as well as the estimated vegetation height from the UAV Digital Elevation Model (DEM) were analysed in terms of tree and weed discrimination and used as input into Random Forest (RF) and k-nearest neighbors (KNN) machine learning algorithms. From the DEM, the Digital Terrain Model (DTM) was estimated using the Inverse Distance Weighted Interpolation (IDW) of the elevation values of dense points on the soil. The plant height was derived by subtracting the DTM from the DEM, resulting in the Canopy Height Model (CHM). The experimental results show that: (i) the combination of spectral bands and the CHM can classify both trees and weeds with an overall accuracy reached 96.87%; (ii) the RF classifier was more robust compared to KNN in the classification performance; (iii) when compared to the use of UAV spectral bands, the addition of the CHM can improve the accuracy of crop classification by 13.36% (KNN) and 1.79% (RF). Furthermore, the integration of UAV imagery in the GEE was highly efficient in terms of automation of the UAV imagery processing.

### 1. Introduction

Weed vegetation is a natural existing component of agroecosystems that develops and spreads rapidly within fields (Dmitriev et al., 2022). Weeds are regarded as the most serious challenge to agricultural crops as they interact with crops for water, nutrients, and light, culminating in yield loss (Shirzadifar et al., 2020). Knowledge and repairing the damage that weeds can produce to a crop during the current or upcoming growing season is critical to effective crop management. The current methods of managing weeds consist of using herbicides for the entire field without considering spatial information about weeds, resulting in economic (exorbitant prices

\* Corresponding author.

E-mail address: [hajar.saadelimanni@usms.ma](mailto:hajar.saadelimanni@usms.ma) (H. Saad El Imanni).

due to overdose), environmental (intense groundwater contamination), and social (herbicide residues in farm products) risks (Su et al., 2022).

Recently, Unmanned Aerial Vehicles (UAVs) have gained prominence as an innovative approach in remote sensing that is useful for managing agriculture practices (Zisi et al., 2018; Kumar et al., 2021). These platforms allow the collection of data with a very high spatial and temporal resolution, which are used for identifying species or levels of stress and diseases (Chang et al., 2020; Neupane and Baysal-gurel 2021), monitoring Forest Health (Dash et al. 2018), detecting individual tree attributes (Gallardo-Salazar and Pompa-García 2020), as well as mapping weed species in early growing season (Shirzadifar et al., 2020; Zaigham Abbas Naqvi et al., 2021).

The contribution of UAV imagery for early season weed identification in crops is based on three major factors: (i) images are flexibly acquired at the most critical agronomic phase for weed management; (ii) the spatial resolution of orthomosaics created from UAV images is very high (<5 cm) as UAV have the ability to fly at low altitudes, thus allowing the detection of plants (trees, crops, and weeds) even at the earliest phenological stage; (iii) dense 3D point cloud derived from UAV images is used to obtain a Digital Surface Model (DSM) (de Castro et al., 2018).

However, it is challenging to automatically differentiate between crops and weeds when only employing ground and UAV spectral bands given the similarity of their spectral signatures (Tamouridou et al., 2017). Many studies have used vegetation canopy height to discriminate vegetation type, map biomass, and identify ecological areas (Zisi et al., 2018). In the USA, weed species were classified using the high resolution of multispectral UAV bands with an overall accuracy of more than 86% (Shirzadifar et al., 2020). In Greece, the spatial distribution of weeds was mapped using spectral bands and plant height generated from UAV images showing an overall accuracy of 95% (Zisi et al., 2018). In Spain, the addition of vegetation indices in the creation of convolutional neural networks for early detection of broad-leaved and grass weeds increased the ability of these models to produce their results with an overall accuracy of around 80% (Torres-Sánchez et al., 2021).

A diversity of classification methods were performed to map weeds from UAV images. In recent years, machine learning algorithms appeared as more accurate alternatives, particularly for large dimensional and complex data (de Castro et al., 2018.). In China, the use of UAV images and Support Vector Machine (SVM) showed to accurately recognize weed species with an overall accuracy of 92.35% (Zhang et al. 2019). In Spain, the evaluation of an automated RF algorithm for early weed mapping using UAV images proved to be robust with an overall accuracy of 87.9% (de Castro et al., 2018).

In Morocco, few studies were performed using the high resolution of multispectral UAV images. Astaoui et al. (2021) used the UAV multispectral images and machine learning to map wheat dry matter, nitrogen content dynamics, and estimation of wheat yield, as well as Marzolff and Kirchhoff. (2019) classified argan trees into various browsing intensities using a UAV remote sensing approach. However, a machine learning approach in the cloud computing environment based on the evaluation of the high resolution of multispectral UAV images for detecting undesired weeds within citrus trees is still not developed in the region.

The aim of this study was:

- To evaluate the potential of single multispectral UAV imagery in the spectral separability of trees and weeds.
- To assess the contribution of the Canopy Height Model (CHM) in the weeds and trees discrimination.
- To evaluate the RF and KNN machine learning techniques in the classification accuracy of trees and weeds land areas, through two experiments:

Experiment 1: weed mapping between and within trees using only RGB bands, near infrared, and red-edge bands

Experiment 2: weed mapping between and within trees using RGB, near infrared, red-edge, and CHM bands

## 2. Materials and methods

### 2.1. Study site and UAV flights

The research location is a citrus farm in the Beni Mellal-Khenifra region of Morocco (central coordinates datum: 32°19'5''N, 6°30'7''W, altitude: 400 m) (Fig. 1). This farm covered an area of about 4.21 ha and was naturally infested by weeds within citrus trees. The fieldwork phase was carried out in the fruit set stage of citrus trees on 1 April 2022 (mid-day on a sunny day). At this stage, also known as the blooming or fruiting stage, the trees produce fruits from their flower sets.

DJI Phantom 4 Multispectral (P4M) quadcopter camera was considered for weed detection within citrus trees (Fig. 1). Multispectral cameras are inexpensive, have high spatial resolution, and are lightweight compared to hyperspectral cameras. As compared to the RGB camera, the multispectral camera has more spectral bands and is less affected by environmental variations due to the presence of a reflectance calibration panel (Su et al., 2022). The P4M camera includes 6 imaging sensors: 5 multispectral sensors (i.e., blue, green, red, red-edge, and near infrared bands) and 1 RGB sensor, both with a global 2 MP shutter. An overview of P4M bands characteristics is presented in Table 1. The sensor size is 4.87 × 3.96 mm, the image size is 1600 × 1300 pixels, and the focal length of the P4M camera is 5.74 mm. The DJI Ground Station Pro application was used to program the flight plan for automatic image acquisition. Flight height was 50 m above ground level (AGL) with a camera angle of 90°, providing 0.024 m/pixel image resolution.

### 2.2. Software for data processing

Agisoft Metashape is the program used to handle UAV data; it is a common photogrammetric processing software for digital images that can process RGB and multispectral images as well as produce photogrammetric products such as DEM and orthomosaic. The GEE platform was considered to analyse the spectral separability of weeds and trees and to map weeds between trees using RF and KNN (Fig. 2).

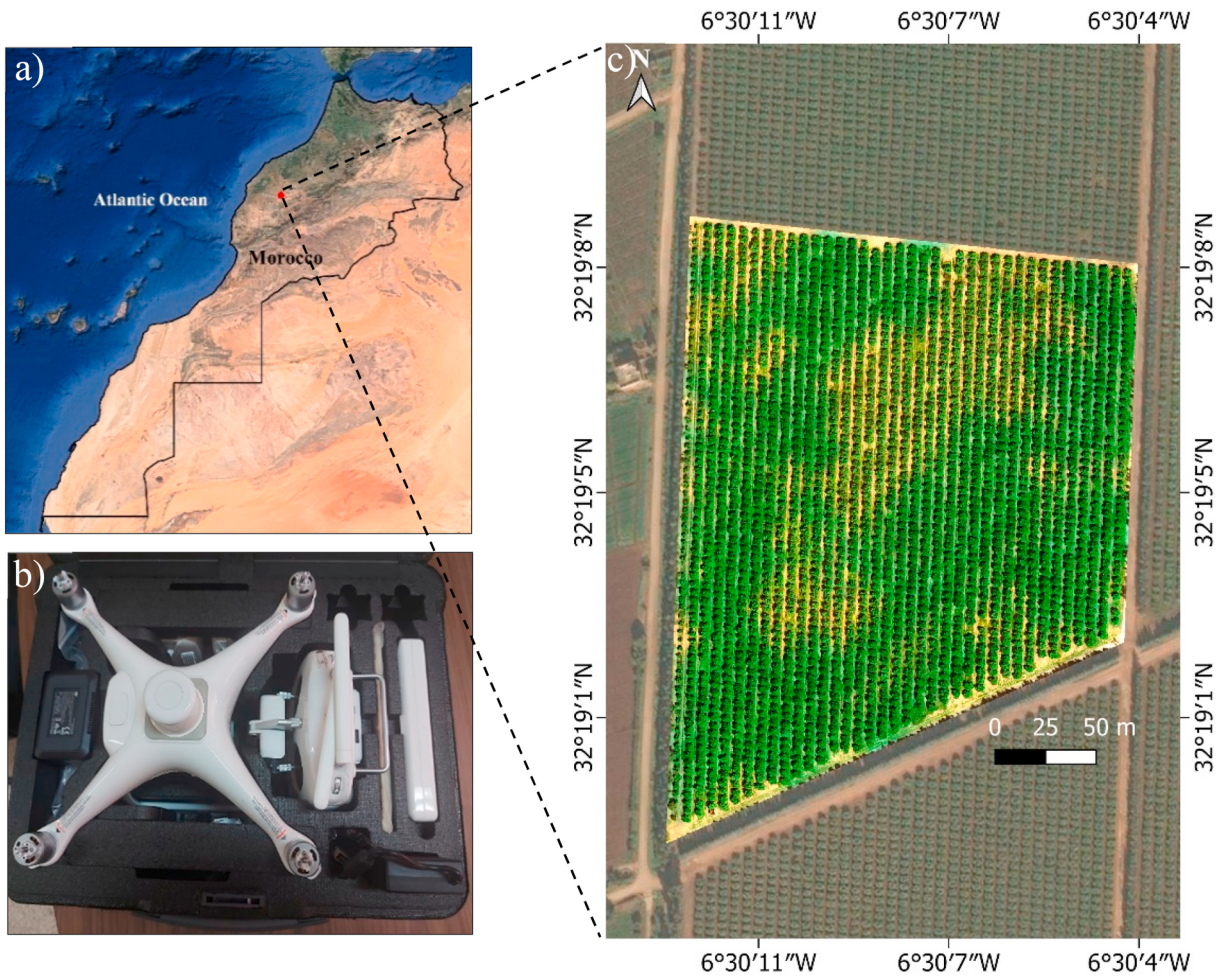


**Fig. 1.** (a) Geographic location of the citrus farm for weed mapping, (b) DJI Phantom 4 Multispectral UAV used for image acquisition, (c) unmanned aerial vehicle (UAV) orthomosaic acquired on 1 April 2022.

**Table 1**

Spectral-band information for (DJI) Phantom 4 Multispectral (P4M).

Band	Central Wavelength (nm)	Wavelength Width (nm)	Band Nu.
Blue	450	32	1
Green	560	32	2
Red	650	32	3
Red-edge	730	32	4
Near-infrared	840	52	5

### 3. Overview of the methodology

An overview of the research process was presented using a flowchart (Fig. 3) that summarizes the following steps: (1) acquisition of UAV images and ground-truth data; (2) generation of dense point clouds, DEM, and ortho-mosaiced image with 1 cm spatial resolution; (3) elaboration of mask shadow; (5) IDW interpolation of soil points, DTM, and CHM deduction; (6) spectral separability between land cover types and classification using RF and KNN.

#### 3.1. Image alignment

The orientation of images, known as 'alignment' in Metashape, is the first step in photogrammetric processing, which is the operation of connecting one image to another. The Agisoft Metashape features detection algorithms (SfM) operate to automatically identify recognizable and characteristic points on each image. The photo alignment returns estimated exterior and interior camera orientation parameters, as well as a sparse point cloud containing triangulated points (Fustinoni et al., 2020) (Fig. 4).

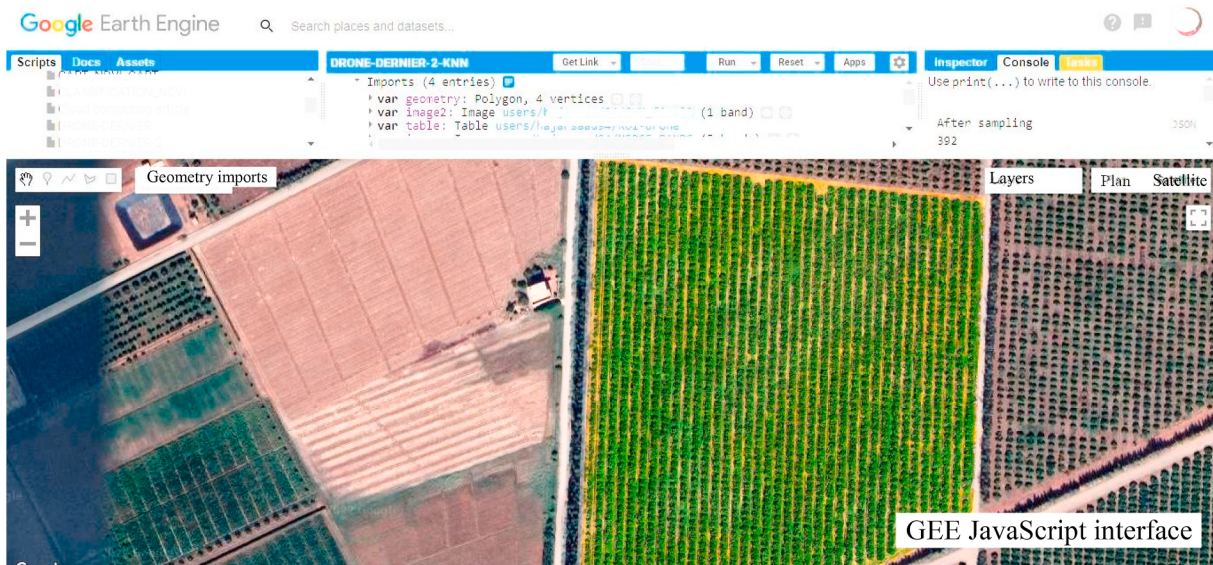


**Fig. 2.** The Google Earth Engine JavaScript interface used for processing the multispectral UAV images.

### 3.2. Digital elevation model (DEM) and orthomosaic

The dense 3D point cloud serves as the foundation for the creation of the detailed digital model. The Digital Elevation Model (DEM) was generated from these points, which allowed height information. The DEM is used as a source surface for the generation of the orthomosaic and reflectance maps of the whole study area, in which every pixel contained RGB, multispectral, and spatial information (Fig. 5).

### 3.3. Canopy Height Model (CHM)

The present research aims to achieve the most accurate classification of trees and weeds, therefore additional features related to height plant information have been treated. The Canopy Height Model (CHM) represents the height or residual distance between the ground and the top of the vegetation above the ground. The CHM is mainly advantageous in classification since the height of individual species is considered and thus provides additional information for their discrimination (Gallardo-Salazar and Pompa-García 2020). This type of use is not practical with the DEM, which contains topographic information for a specific study area. The CHM was deduced by subtracting the Digital Terrain Model (DTM) from the Digital Surface Model (DSM) or DEM.

Therefore, to generate the CHM of the study area, it was required to perform a representative surface interpolation of the ground for subtracting it from the DEM. Many studies showed that the interpolation method used in generating the DTM is the kriging method (Erdede and Bektaş 2020). As a result, the kriging interpolation method was used to have a representative surface of the ground.

### 3.4. Shadow removing

Shadow detection and removal in images are constantly significant challenge that reduces the accuracy of information. In the study site, the shadow areas were formed on the side opposite the solar radiation of the citrus trees. Thresholding is a commonly used technique for shadow detection, in which a threshold value is chosen to differentiate between regions with and without shadows (Anoopa et al. 2016). In this study, a manual shadow thresholding mask was applied, as the reflectance values in the shadow areas are very distinct in the near infrared band, the shadow pixels were masked by using a threshold of reflectance values  $< 0.009$  in the near infrared band, to remove pixels that were observed to be shadows (Fig. 6).

### 3.5. Image classification and accuracy assessment

In this study, two machine learning algorithms were evaluated in weed mapping between citrus trees. As described by (Breiman 2001), the Random Forest (RF) algorithm is an ensemble of various decision trees, with each tree contributing a single vote for the most prevalent class (Adam et al., 2014). Building a collection of Decision Trees (DTs) allows the RF classifier to overcome the overfitting issue with DT classifiers, resulting to a more robust classifier (Breiman 2001). Practically, RF creates a number of DT classifiers for each tree that are used for training and producing classes (Shelestov et al., 2017).

The K-Nearest Neighbor (K-NN) is a classification technique that is included in the supervised algorithms, and easily applied to solve classification and regression cases. The KNN algorithm is used to classify data by determining the value of group k for the object in the training set that is most similar to the object in the testing set (Saputra et al., 2020). The KNN algorithm is typically used to calculate the distance between two objects using the following euclidean distance statistics formula:

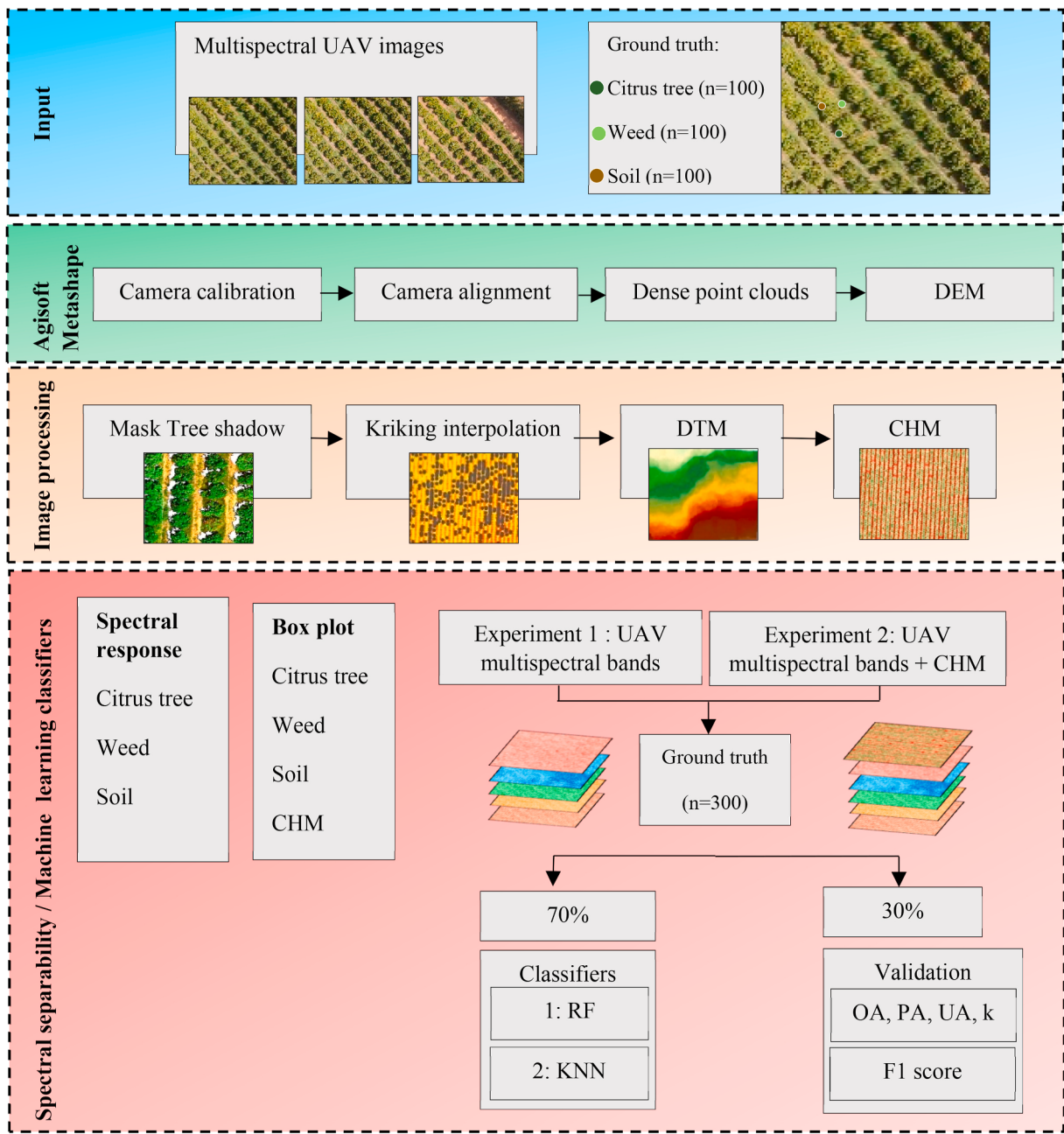


Fig. 3. Flowchart of the proposed methodology.

$$d(x, y) = \sqrt{\sum_{i=1}^n (x_i - y_i)^2}$$

Note.

- $d(x,y)$ : the distance between testing and training data;
- $x$ : data testing;
- $y$ : data training;
- $n$ : the amount of training data.

Five confusion metrics, including overall accuracy (OA), Kappa coefficient, user accuracy (UA), producer accuracy (PA), and F1 score, were used to evaluate the accuracy of the classification result. For training purposes, 70% of the ground truth for each class was

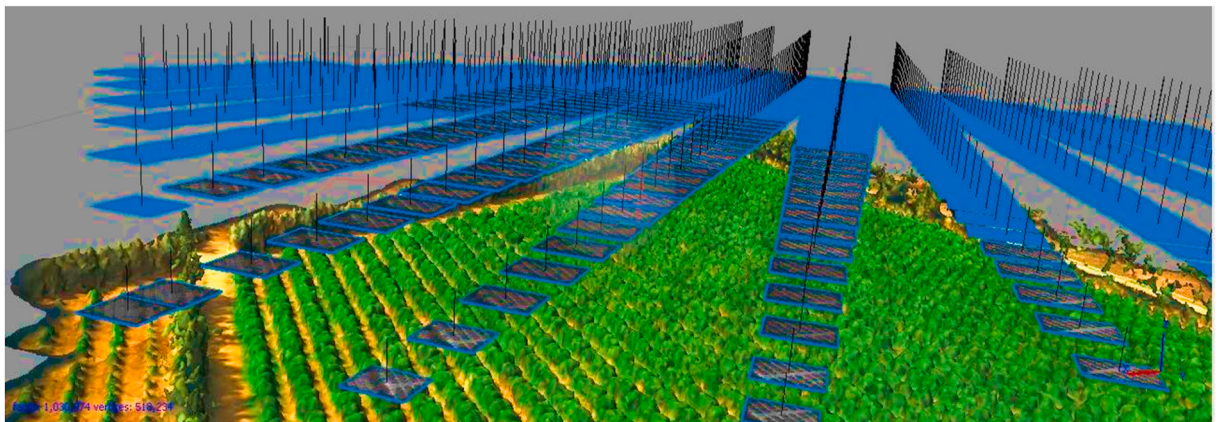


Fig. 4. Screenshot on some aligned images on Metashape.

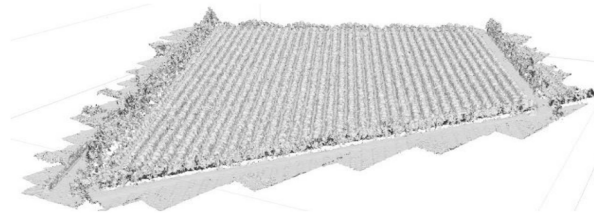


Fig. 5. Dense point cloud obtained from processing the UAV images.

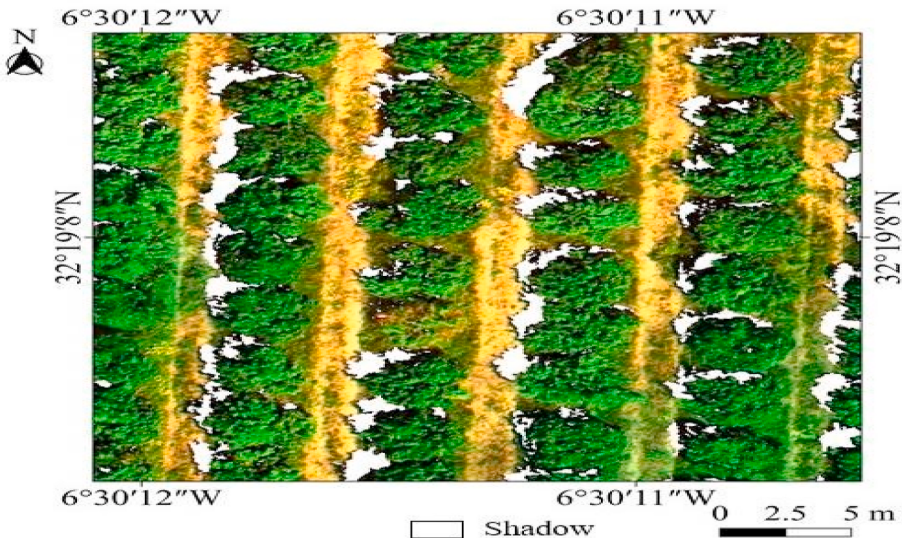


Fig. 6. A detailed zoom of shadows masking.

randomly selected for training, while the remaining 30% of ground survey sites were used to evaluate the accuracy of classification. The OA was obtained by adding the number of properly categorized cells and dividing by the total number of cells, while the Kappa coefficient assesses the percentage of errors that are reduced by classification compared to purely random classification (Hudait and Patel 2022; Saad El Imanni et al., 2022).

The PA is the conditional probability that a specific position on the classification map's output will match any random sample in the test data, while the UA selects a random sample with the same conditional probability as the real type of ground from the classification results (Luo et al., 2021). The PA and UA were derived from the error matrix of classification.

The harmonic mean of PA and UA is calculated using the F1 score, which is a significant metric for balancing the difference between PA and UA for each class (Aduvukha et al., 2021). These accuracies were calculated based on the equations below.

$$OA (\%) = \frac{\sum_{i=1}^n p_{ii}}{N} \times 100$$

$$Kappa = \frac{N \sum_{i=1}^n p_{ii} - \sum_{i=1}^n (p_{i+} \times p_{+i})}{N^2 - \sum_{i=1}^n (p_{i+} \times p_{+i})}$$

$$UA (\%) = \frac{p_{ii}}{p_{i+}} \times 100$$

$$PA (\%) = \frac{p_{ii}}{p_{+i}} \times 100$$

$$F1 score (\%) = \frac{UA \times PA}{UA + PA} \times 2$$

Note.

- $n$  is the total number of columns of the confusion matrix;
- $p_{ii}$  is the number of correct classifications of the upper crop-type sample in the  $i$  row and  $i$  column of the confusion matrix;
- $p_{i+}$  and  $p_{+i}$  are the total number of crop-type samples in row  $i$  and column  $i$ ;
- $N$  is the total number of samples used for verification.

### 3.6. Experimental design

In view of evaluating the band reflectance values, the height information, and the performance of RF and KNN machine learning classifiers in weed mapping between and within trees, two experiments were designed.

*Experiment 1:* The UAV multispectral bands were used as input to the RF and KNN classification.

*Experiment 2:* The UAV multispectral bands, as well as the height information, were used as input to the RF and KNN classification.

## 4. Results

### 4.1. Results of UAV flights

The multispectral camera generated 414 RGB, RedEdge, and NIR images. Figs. 7 and 8 show the image results from processing the collected images. Following processing the orthomosaic bands, which had 16-bit integer values, the normalized reflectance was returned in the range of 0–1. Since 100% of the reflectance for each band matches the middle of the available range, i.e. 32768, the output bands were edited by dividing the original values by the normalization factor (32,768). The obtained products have an area of 4.21 ha and a spatial resolution of 0.024 m.

Elevation information taken from the DEM was attributed to 1590 points and the Kriging interpolation was performed to deduce the DTM values. The resulting DTM surface, which was thought to be representative of the soil plane was subtracted from the original DEM to generate the CHM (Fig. 8).

### 4.2. Spectral separability

In this section, a spectral analysis was performed, with the mean reflectance values of the spectral bands for the tree, weed, and soil land cover classes (Fig. 9). The spectral profile of tree and weed classes corresponds to the typical spectral profile of the photosynthetic vegetation, showing lower values in the RGB bands (B1, B2, and B3) and higher values in the NIR and red-edge bands (B4, B5). In comparison to the tree class, the weed class exhibited greater values in the B1, B2, and B5 bands. Assessing the soil reflectance profile to that of weed and tree classes revealed greater values in the B1, B2, and B3 bands and lower values in the B4 and B5 bands.

Fig. 10 shows the boxplots of the statistical analysis of the spectral response of trees, weeds, and soil. The spectral response distribution of citrus tree, weed, and soil revealed that the citrus tree boxplot represented the lowest median spectral response in the visible bands, while it showed the greater median spectral response in the near infrared. The citrus tree class showed a much larger distribution than weed and soil classes, as within this class there was a variety in the phenological condition, as healthy and stressed trees. For the B3 band, the interquartile ranges of citrus tree, weed, and soil were 0.02–0.05 (citrus tree), 0.03–0.04 (weed), and 0.12–0.15 (soil), while the interquartile ranges for the B5 band were 0.27–0.43 (citrus tree), 0.31–0.44 (weed), and 0.17–0.21 (soil).

Fig. 11 shows the height statistical analysis of the training data per class. For DEM, the interquartile ranges of citrus tree, weed, and soil were 436.90 m–438.64 m, 434.98 m–435.78 m, and 434.98 m–435.74 m, respectively. For CHM, citrus tree and weed classes showed notably higher trends, 2.69 m–3.08 m and 0.02 m–0.07 m, respectively. Table 2 resumes the height statically results of the training data per class.

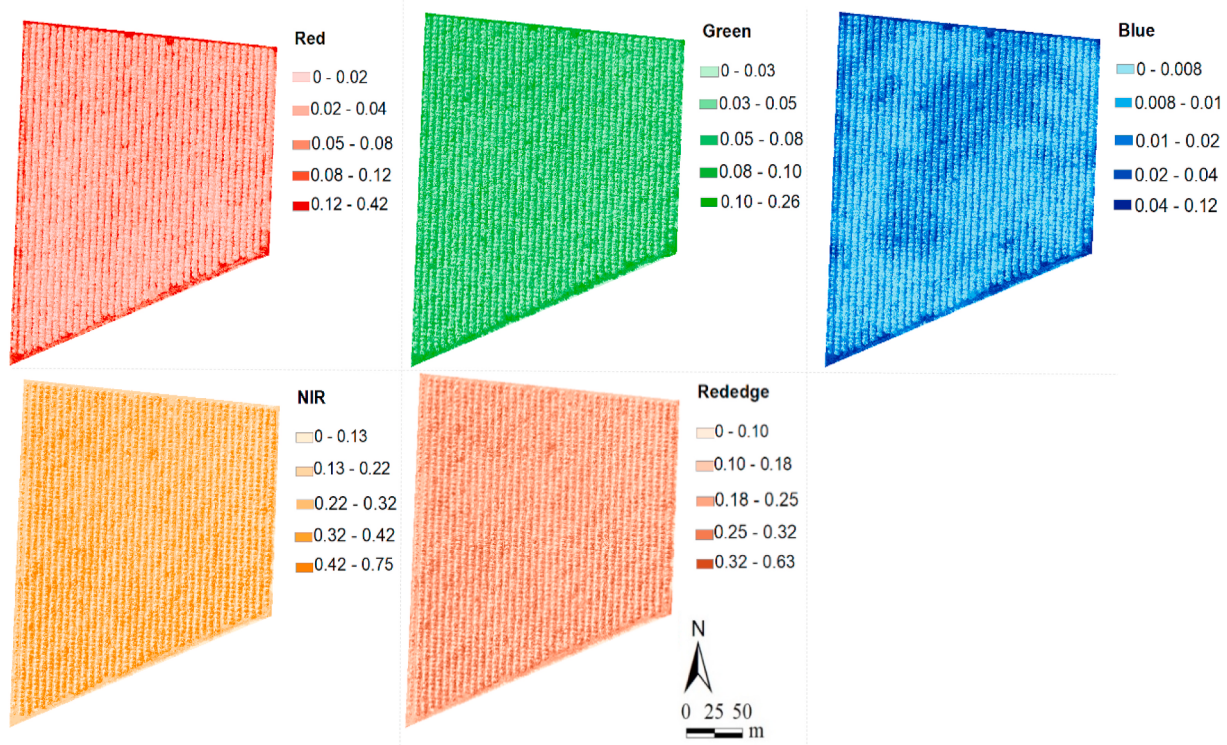


Fig. 7. Multispectral bands generated from processing the collected UAV images.

#### 4.3. Weed detection

Four maps showing the distribution of weeds, trees, and soil were produced from the execution of the RF and KNN classification techniques on two combinations of input data layers (Figs. 12 and 13). The produced maps revealed that the study area is naturally infested by important patches of weeds within citrus trees.

As shown in Fig. 14, the classification accuracy of experiment 2 ( $OA = 96.87\%$ ,  $k = 0.95$  (RF), and  $OA = 93.75\%$ ,  $k = 0.90$  (KNN)) is higher than that of experiment 1 ( $OA = 95.08\%$ ,  $k = 0.92$  (RF), and  $OA = 80.39\%$ ,  $k = 0.69$  (KNN)), which demonstrates that the addition of the CHM band to the multispectral UAV images improve the crop classification accuracy (the difference between the lowest and the highest accuracies is 1.79% (RF) and 13.36% (KNN)). In all experiments, the RF obtained the best classification performance compared to KNN.

Table 3 highlights the summary of error matrices generated during the accuracy assessment of the resulting maps, demonstrating the following performance metrics: overall classification accuracy, Kappa statistic, user's accuracy, and producer's accuracy for the three landcover classes. The overall accuracy of experiment 1 was lower when using the KNN classifier ( $OA = 80.39\%$ ,  $k = 0.69$ ), while the RF classifier performed better than the KNN ( $OA = 96.87\%$ ,  $k = 0.95$ ). For the two pixel-based classifiers, higher accuracy levels were achieved with the fusion of spectral bands (RGB, near infrared, and red edge) and height information (CHM).

Assessing the user's and producer's accuracies between the two classifiers, lower weed user's accuracies were consistently observed for KNN when using only spectral bands as input to the classification. This is due to the high levels of commission errors observed because of the high number of false positives (overestimation) of other vegetation class. This finding can be attributed to the KNN classifier's failure to account for class spectral variance. However, when using the RF classifier the weed user accuracy was performed to 92%.

The use of plant height information additionally resulted in greater accuracy, with the highest user and producer accuracy reaching 100% and 100% (citrus tree), 100% and 86% (weed), and 90% and 100% (soil).

As a result of training the RF model using all 6 variables (Fig. 15), variable importance indicated that the two most important variables to the classification were CHM (importance = 33.65%) and B3 (importance = 22.62%), while B4 had the lowest importance (importance = 4.13%).

#### 4.4. Weed area forecasting

In this section, the resulting image of RF classification from the fusion of spectral and height data (experiment 2) was investigated to estimate the land cover classes. The area of citrus tree, weed, and soil classes is calculated by multiplying the number of pixels classified into a class by the area of each pixel (Table 4). The obtained area of weed was 1.22 ha representing 28% of the study area.

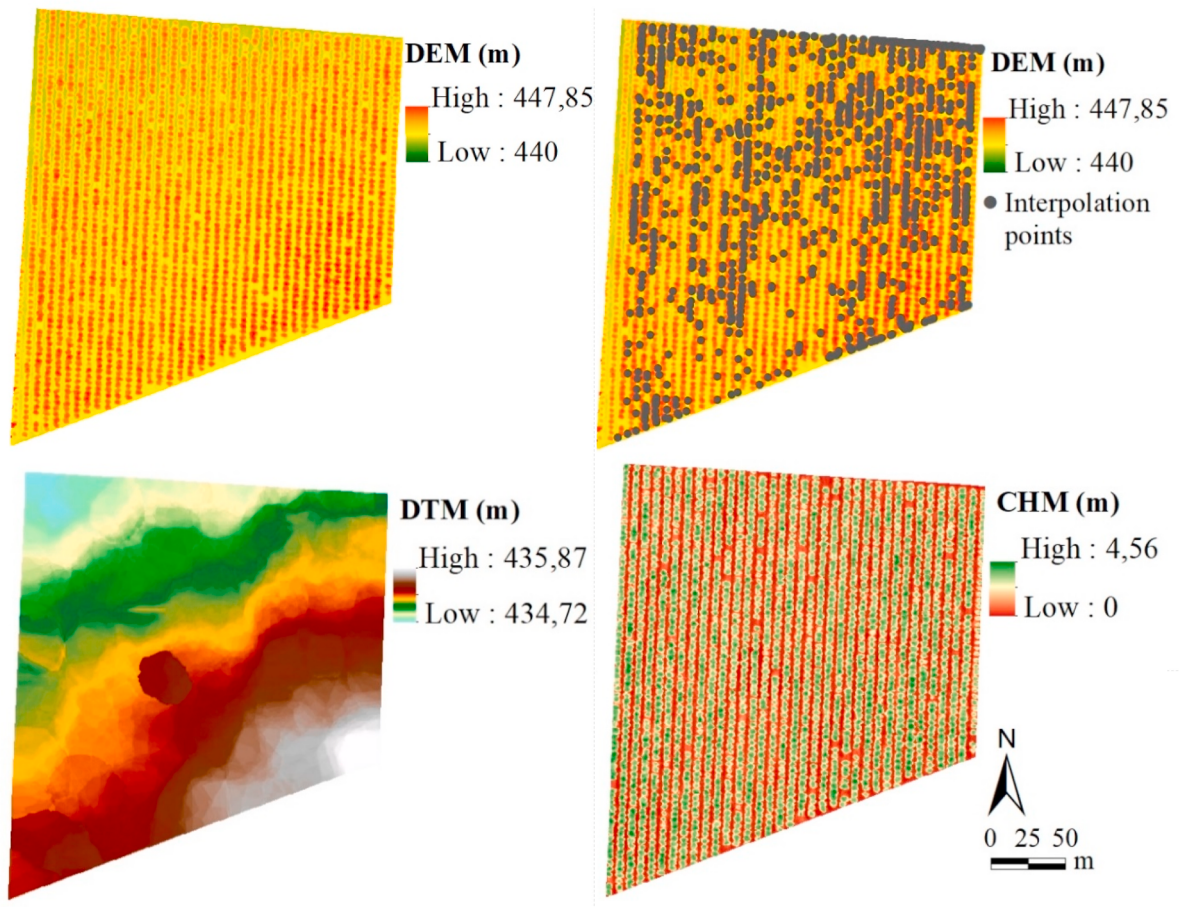


**Fig. 8.** Height information derived from processing the collected UAV images.

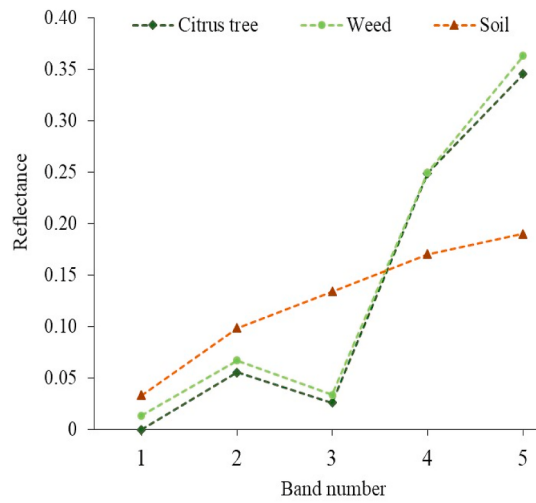


**Fig. 9.** Mean Spectral profiles of citrus tree, weed, and soil for UAV multispectral bands.

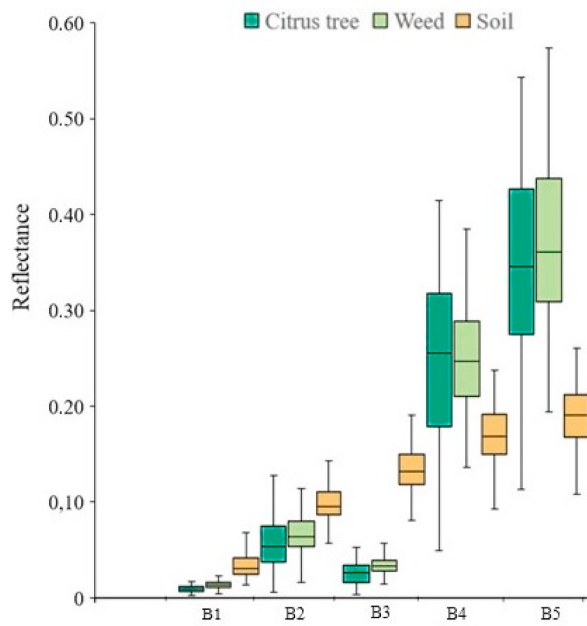


**Fig. 10.** Boxplots of UAV multispectral bands values of land cover classes.

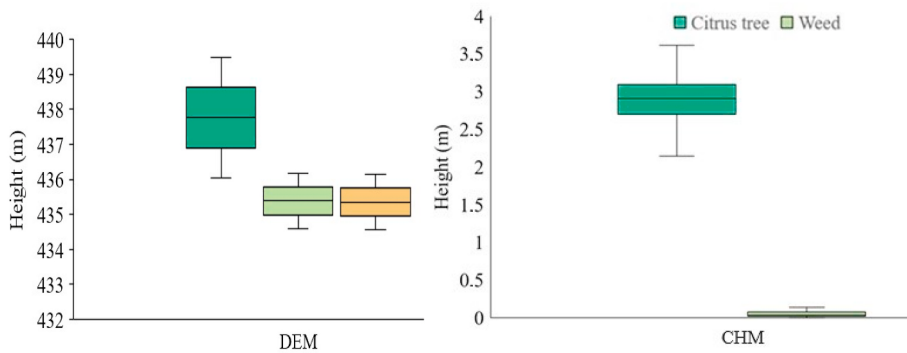


**Fig. 11.** Boxplots of UAV height data characteristics of land cover classes.

**Table 2**  
Height information of training data per class.

CHM	Min	Max	Median
Citrus tree	1.86 m	3.89 m	2.90 m
Weed	0.03 m	0.32 m	0.04 m

## 5. Discussion

### 5.1. Discussion

The research paves the path for a new cloud computing approach based on the incorporation of multispectral UAV imagery in the GEE programming environment for analysing and improving the separation accuracy of trees and weeds in a citrus farm for sophisticated image processing and analysis.

Weed mapping between and within trees is challenging due to the similarity of spectral response. As a result, this study involved five multispectral bands, as well as the elevation information (DEM) derived from the UAV multispectral images as inputs into RF and KNN classifiers to accurately classify trees and weeds. To 1590 points, terrain elevation data from the DEM was added. The DTM values were attributed using the Kriging interpolation technique. The obtained DTM surface, which was believed to be representative of the soil plane across the entire area, was then subtracted from the initial DEM to produce the CHM.

Results revealed that the spectral profiles as well as the statistical boxplots of the citrus tree and weed classes showed close distributions in all spectral bands, while the height analysis revealed notably higher trends, 2.69 m–3.08 m (citrus tree) and 0.02 m–0.07 m

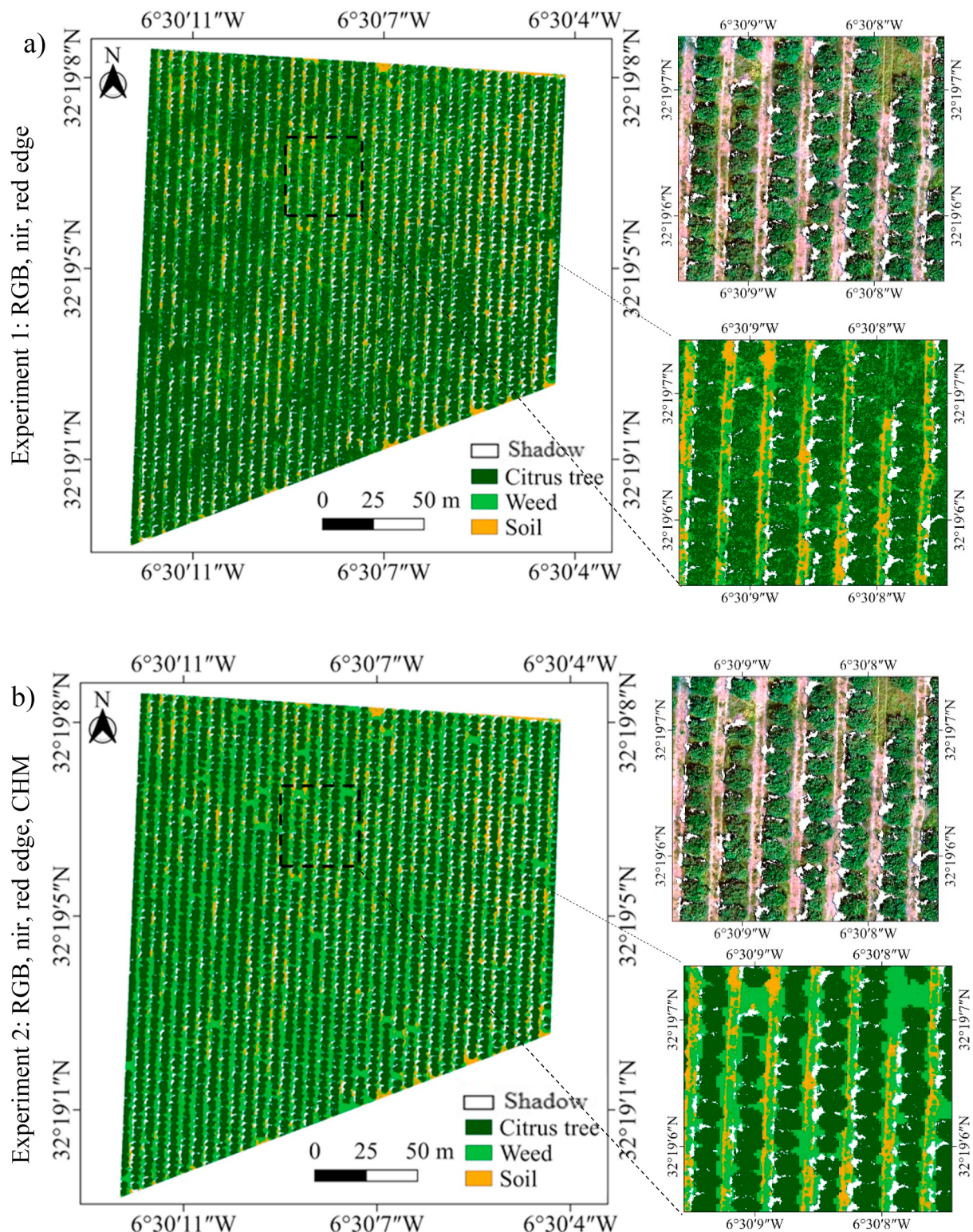


Fig. 12. Results of applying the RF model to the study area: (a) RF result based on experiment 1, (b) RF result based on experiment 2.

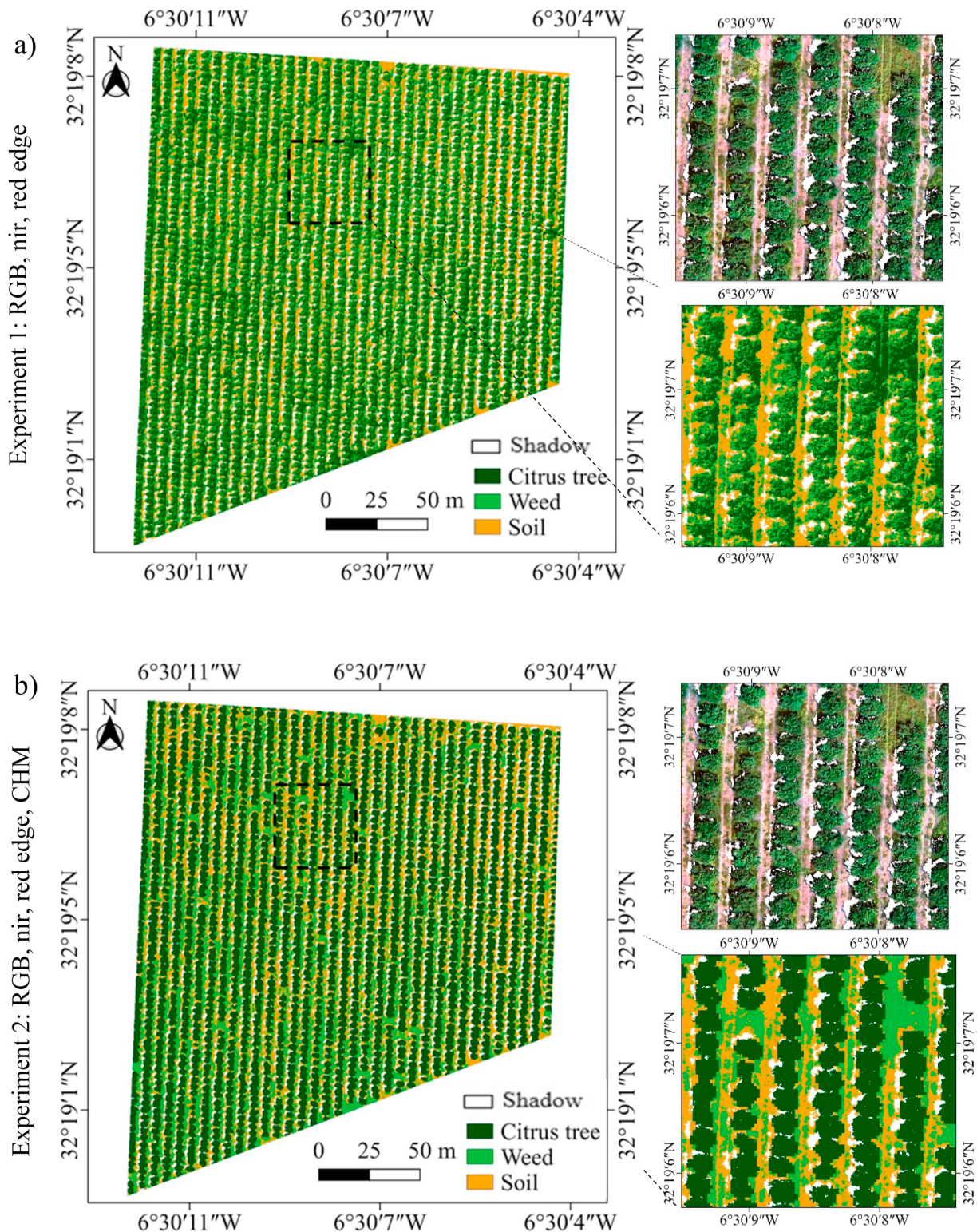


Fig. 13. Results of applying the KNN model to the study area: (a) RF result based on texperiment 1, (b) RF result based on experiment 2.

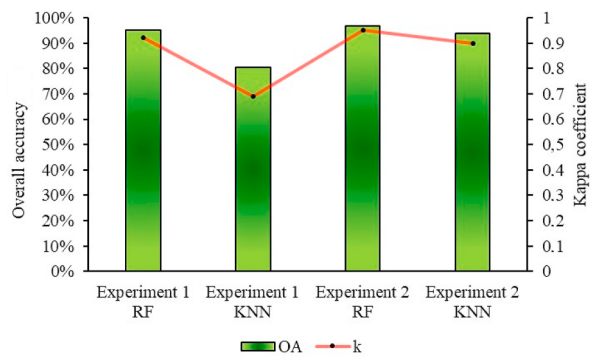


Fig. 14. Classification accuracy of experiments using RF and KNN models.

**Table 3**

Confusion matrix for the RF and KNN results.

Input Data	Overall Acc. (%)	Kappa coefficient	User's Acc. (Tree) (%)	Producer's Acc. (Tree) (%)	User's Acc. (Weed) (%)	Producer's Acc. (Weed) (%)	User's Acc. (Soil) (%)	Producer's Acc. (Soil) (%)
RGB, nir, red edge (RF)	95.08	0.92	97	97	92	92	95	95
RGB, nir, red edge (KNN)	80.39	0.69	92	84	54	54	54	81
RGB, nir, red edge, CHM (RF)	96.87	0.95	100	100	100	86	90	100
RGB, nir, red edge, CHM (KNN)	93.75	0.90	100	100	100	71	81	100

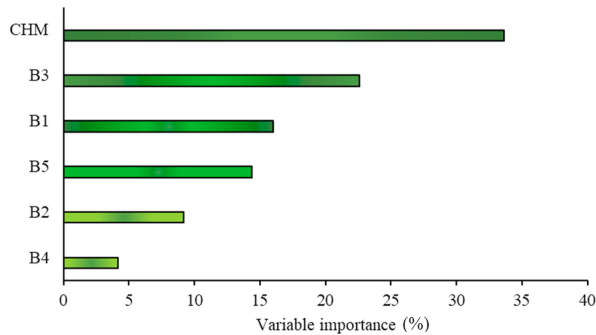


Fig. 15. Variable importance as a result of training the RF model using all 6 variables (experiment 2).

(weed). In essence, the CHM used height measurements to distinguish between trees and weeds. This outcome might serve as a guide for farmers to determine the dosages of herbicides to apply in the field's treatment areas (Stroppiana et al., 2018).

According to the results of experiments, experiment 1 (RGB, near infrared, red edge) generate an accurate classification when using the RF classifier (OA = 95.08% and k = 0.92) compared to KNN classifier (OA = 80.39% and k = 0.69). This finding is in accordance with previous studies, which demonstrated the robustness of RF compared to other machine learning algorithms in crop classification (Zhu et al., 2019).

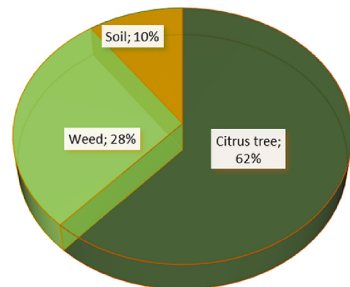
The performance of weed mapping was significantly enhanced by the incorporation of the elevation data (CHM), increasing the overall accuracy from 95.08% to 96.87.5% for RF and from 80.39% to 93.75% for KNN and the k statistic from 0.92 to 0.95 for RF and 0.69 to 0.9 for KNN. This result is consistent with Zisi et al. (2018) study, which revealed that the incorporation of the surface elevation information in UAV images improves the accuracy of weed patches mapping.

Fig. 16 shows that the F1 score of the citrus tree and weed improved when the CHM information was incorporated to the spectral bands. In the KNN classification result, the weed classification accuracy was lower when only spectral bands were employed (F1 score = 54%), however, it was enhanced when the CHM band was added to these bands (F1 score = 83.04%). The RF classifier produced a high F1 score (92%) for the accuracy of the weed classification when using only spectral bands (F1 score = 92%).

These findings demonstrate that the KNN classifier requires the incorporation of CHM in order to classify weeds. However, the RF classifier was able to accurately classify the weeds using only the multispectral bands, with a 0.47% improvement after adding CHM. In Greece, Zisi et al. (2018) compared the accuracy of spectral bands and texture with the accuracy of spectral bands and height data, finding that the best accuracy was achieved when plant height data were used as input.

**Table 4**

The number of pixels and estimated area based on the RF classification and experiment 2, on 1 April 2022.



Landcover classes	Number of pixels	Estimated Area (ha)
Citrus tree	3219824	2.60
Weed	1513843	1.22
Soil	478,851	0.39

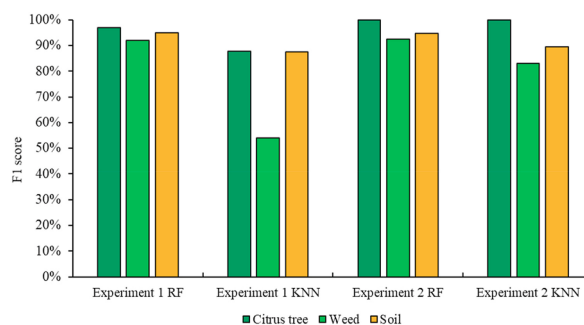


**Fig. 16.** F1 score of citrus tree, weed, and soil as a function of experiments and RF, KNN models.

This study also emphasized the value of mask shadow for the UAV images processed during the pre-processing steps, as a way to achieve accurate results. [De Castro et al. \(2018\)](#) performed an automatic Random Forest-OBIA Algorithm with shadow removing for weed detection.

The information on plant height is believed to be an adequate improvement of the classification accuracy of weeds between and within trees, between and within trees. The height of the plant information could be useful to other weed species and crop mixtures ([Zisi et al., 2018](#)). The combination of multispectral UAV imagery, plant height information, machine learning algorithms, and the cloud computing interface allow rapid and accurate weed detection, between and within trees. This could assist farmers in the decision-making process and repairing the damage that weeds can produce to a crop at the early stage.

## 5.2. Limitations and future research

In this study, we only used vegetation height plants as additional information with UAV multispectral bands to improve the weed mapping between and within trees. However, this information may not be enough suitable for detecting weeds between crops. As a result, in future research authors recommended using of other supplementary layers such as plant texture and color. In this work, RF and KNN algorithms were evaluated in weed mapping, therefore the authors encourage the consideration of other machine learning algorithms for more accurate weed mapping.

## 6. Conclusion

The application of UAV technologies and cloud computing in agricultural policy and practice is still in its infancy in this region. This was the first time that multispectral bands and height information derived from UAV images were employed to detect weeds between and within trees using machine learning algorithms, such as the RF and KNN.

In this study, the spectral separability of trees and weeds was examined using UAV multispectral bands, and the height of these plants was determined by calculating the CHM, which revealed a height of 2.69 m–3.08 m (citrus tree) and 0.02 m–0.07 m (weed).

The weed mapping was achieved with high accuracy using UAV images and an additional secondary layer of information related to plant height (CHM). The performance of weed mapping was significantly enhanced by the incorporation of the height plant data (CHM) to the multispectral bands, increasing the overall accuracy from 95.08% to 96.87.5% for RF and from 80.39% to 93.75% for KNN.

Furthermore, the cloud computing approach was highly efficient in terms of computation and time reduction. The findings from this study can be applied to other weed and crop combinations with significant height differences.

## Funding

This research received no external funding.

## Ethical statement

I declare, in conjunction with my coauthors, that all ethical practices in relation to the development, writing and publishing of this paper have been reviewed and followed.

## Declaration of competing interest

The authors declare that they have no known competing financial interests or personal relationships that could have appeared to influence the work reported in this paper.

## Data availability

The authors do not have permission to share data.

## Acknowledgments:

We gratefully acknowledge the anonymous referees for their helpful revisions and remarks.

## References

- Adam, E., Mutanga, O., Odindi, J., Abdel-Rahman, E.M., 2014. Land-use/cover classification in a heterogeneous coastal landscape using RapidEye imagery: evaluating the performance of random forest and Support vector machines classifiers. *Int. J. Rem. Sens.* 35 (10), 3440–3458.
- Aduvukha, G.R., Abdel-Rahman, E.M., Sichangi, A.W., Makokha, G.O., Landmann, T., Mudereri, B.T., Tonnang, H.E.Z., Dubois, T., 2021. Cropping pattern mapping in an agro-natural heterogeneous landscape using sentinel-2 and sentinel-1 satellite datasets. *Agriculture* 11 (6), 1–22.
- Anoopa, S., Dhanya, V., Kizhakkethottam, J.J., 2016. Shadow detection and removal using tri-class based thresholding and shadow matting technique. *Procedia Technol.* 24, 1358–1365. <https://doi.org/10.1016/j.protcy.2016.05.148>.
- Astaoui, G., Dadaiss, J.E., Sebiri, I., Benmansour, S., Mohamed, E., 2021. Mapping wheat dry matter and nitrogen content dynamics and estimation of wheat yield using UAV multispectral imagery machine learning and a variety-based approach: case study of Morocco. *AgriEngineering* 3 (1), 29–49.
- Breiman, L., 2001. Statistical modeling: the two cultures. *Stat. Sci.* 16 (3), 199–215.
- de Castro, A.I., Torres-Sánchez, J., Peña, J.M., Jiménez-Brenes, F.M., Csillik, O., López-Granados, F., 2018. An automatic random forest-OBIA algorithm for early weed mapping between and within crop rows using UAV imagery. *Rem. Sens.* 10 (2).
- Chang, A., Yeom, J., Jung, J., Landivar, J., 2020. Comparison of canopy shape and vegetation indices of citrus trees derived from uav multispectral images for characterization of citrus greening disease. *Rem. Sens.* 12 (24), 1–12.
- Dash, J.P., Pearse, G.D., Watt, M.S., 2018. UAV multispectral imagery can complement satellite data for monitoring forest Health. *Rem. Sens.* 10 (8), 1–22.
- Dmitriev, P.A., Kozlovsky, B.L., Kupriushkin, D.P., Dmitrieva, A.A., Rajput, W.D., Chokheli, V.A., Tarik, E.P., et al., 2022. Assessment of invasive and weed species by hyperspectral imagery in agrocenoses ecosystem. *Rem. Sens.* 14 (10). 2442.
- Erdede, S.B., Bektaş, S., 2020. Examining the interpolation methods used in forming the DiErdede, S.B., and S. Bektaş. 2020. Examining the interpolation methods used in forming the digital elevation models. *Celal Bayar Univers.J.Sci.* 16 (2), 207–214. . Gital Elevation Mod, Gital Elevation Mod. Celal Bayar University Journal of Science 16, no. 2: 207–214.
- Gallardo-Salazar, J.L., Pompa-García, M., 2020. Detecting individual tree attributes and multispectral indices using unmanned aerial vehicles: applications in a pine clonal orchard. *Rem. Sens.* 12 (24), 1–22.
- Hudait, M., Patel, P.P., 2022. Crop-type mapping and acreage estimation in smallholding plots using sentinel-2 images and machine learning algorithms: some comparisons. *Egypt. J. Rem. Sens. Space Sci.* 25 (1), 147–156. <https://doi.org/10.1016/j.ejrs.2022.01.004>.
- Kumar, A., Desai, S.V., Balasubramanian, V.N., Rajalakshmi, P., Guo, W., Balaji Naik, B., Balram, M., Desai, U.B., 2021. Efficient maize tassel-detection method using UAV based remote sensing. *Remote Sens. Appl.: Soc. Environ.* 23. <https://doi.org/10.1016/j.rsase.2021.100549>. May: 100549.
- Luo, C., Liu, H., Lu, L., Liu, Z., Kong, F., Zhang, X., 2021. Monthly composites from sentinel-1 and sentinel-2 images for regional major crop mapping with Google Earth engine. *J. Integr. Agric.* 20 (7), 1944–1957. [https://doi.org/10.1016/S2095-3119\(20\)63329-9](https://doi.org/10.1016/S2095-3119(20)63329-9).
- Marzolff, I., Kirchhoff, M., 2019. UAV-based Remote Sensing in Argan Woodlands , Morocco UAV-Based Remote Sensing in Argan Woodlands. (Morocco, January).
- Neupane, K., Baysal-gurel, F., 2021. Automatic Identification and Monitoring of Plant Diseases Using Unmanned Aerial Vehicles : A Review.
- Saad El Imanni, H., El Harti, A., Hssaisoune, M., Velastegui-Montoya, A., Elbouzidi, A., Addi, M., El Iysaouy, L., El Hachimi, J., 2022. Rapid and automated approach for early crop mapping using sentinel-1 and sentinel-2 on Google Earth engine; A case of a highly heterogeneous and fragmented agricultural region. *J. Imag.* 8 (12).
- Saputra, R.A., Suharyanto, W., Saefudin, D.F., Supriyatna, A., Wibowo, A., 2020. Rice leaf disease image classifications using KNN based on GLCM feature extraction. *J. Phys. Conf.* 1641 (1).
- Shelestov, A., Lavreniuk, M., Kussul, N., Novikov, A., Skakun, S., 2017. Exploring Google Earth engine platform for big data processing: classification of multi-temporal satellite imagery for crop mapping. *Front. Earth Sci.* 5 . February: 1–10.
- Shirzadifar, A., Bajwa, S., Nowatzki, J., Bazrafkan, A., 2020. Field identification of weed species and glyphosate-resistant weeds using high resolution imagery in early growing season. *Biosyst. Eng.* 200, 200–214. <https://doi.org/10.1016/j.biosystemseng.2020.10.001>.
- Stroppiana, D., Villa, P., Sona, G., Ronchetti, G., Candiani, G., Pepe, M., Busetto, L., Migliazza, M., Boschetti, M., 2018. Early season weed mapping in rice crops using multi-spectral UAV data. *Int. J. Rem. Sens.* 39 (15–16), 5432–5452. <https://doi.org/10.1080/01431161.2018.1441569>.
- Su, J., Yi, D., Coombes, M., Liu, C., Zhai, X., McDonald-Maier, K., Chen, W.H., 2022. Spectral analysis and mapping of blackgrass weed by leveraging machine learning and UAV multispectral imagery. *Comput. Electron. Agric.* 192, 106621. <https://doi.org/10.1016/j.compag.2021.106621>. March 2021.
- Tamouridou, A.A., Alexandridis, T.K., Pantazi, X.E., Lagopodi, A.L., Kashefi, J., Moshou, D., 2017. Evaluation of UAV imagery for mapping silybum marianum weed patches. *Int. J. Rem. Sens.* 38 (8–10), 2246–2259. <https://doi.org/10.1080/01431161.2016.1252475>.
- Torres-Sánchez, J., Mesas-Carrascosa, F.J., Jiménez-Brenes, F.M., de Castro, A.I., López-Granados, F., 2021. Early detection of broad-leaved and grass weeds in wide row crops using artificial neural networks and UAV imagery. *Agronomy* 11 (4).
- Zaigham Abbas Naqvi, S.M., Awais, M., Khan, F.S., Afzal, U., Naz, N., Khan, M.I., 2021. Unmanned air vehicle based high resolution imagery for chlorophyll estimation using spectrally modified vegetation indices in vertical hierarchy of citrus grove. In: *Remote Sensing Applications*, vol. 23. Society and Environment. <https://doi.org/10.1016/j.rsase.2021.100596>. May: 100596.
- Zhang, S., Guo, J., Wang, Z., 2019. Combing K-means clustering and local weighted maximum discriminant projections for weed species recognition. *Front. Comput. Sci.* 1 (September), 1–11.
- Zhu, J., Pan, Z., Wang, H., Huang, P., Sun, J., Qin, F., Liu, Z., 2019. An improved multi-temporal and multi-feature tea plantation identification method using sentinel-2 imagery. *Sensors* 19 (9).

Zisi, T., Alexandridis, T.K., Kaplanis, S., Navrozidis, I., Tamouridou, A.A., Lagopodi, A., Moshou, D., Polychronos, V., Zisi, T., Alexandridis, T.K., Kaplanis, S., Navrozidis, I., Tamouridou, A.A., Lagopodi, A., Moshou, D., Polychronos, V., 2018. Incorporating surface elevation information in UAV multispectral images for mapping weed patches. 2018. J. Imag. 4 (11). . Inco. *Journal of Imaging* 4, no. 11.